DATE: 28 February 2011

Foreign Object Damage Prediction in Ceramic Matrix Composites

Prepared for:
NAVAIR
47123 Buse Road, Building 2188, Floor 1, Room 101A
Patuxent River, MD 20670

Mr. Ian Miller (N&R Engineering)

Dr. Vinod Nagpal (N&R Engineering)

Dr. Erdogan Madenci (University of Arizona)

20110304337

REPORT DOCUMENTATION PAGE

Form Approved
OMB No. 0704-0188

1. REPORT DATE *(DD-MM-YYYY)*
02/28/2011

2. REPORT TYPE
Final

3. DATES COVERED *(From - To)*
7/30/2010 - 02/28/2011

4. TITLE AND SUBTITLE
Analysis and Modeling of Foreign Object Damage (FOD) in Ceramic Matrix Composites (CMCs)

5a. CONTRACT NUMBER
N68335-10-C-0420

5b. GRANT NUMBER
NA

5c. PROGRAM ELEMENT NUMBER
NA

6. AUTHOR(S)
Miller, Ian
Mandenci, Erdogan

5d. PROJECT NUMBER
1300156296

5e. TASK NUMBER
N10A-010-0559

5f. WORK UNIT NUMBER
NA

7. PERFORMING ORGANIZATION NAME(S) AND ADDRESS(ES)
N&R Engineering
6659 Pearl Road, Suite 201
Parma Heights, OH 44130

University of Arizona
1130 N. Mountain
Tucson, AZ 85721

8. PERFORMING ORGANIZATION REPORT NUMBER
1

9. SPONSORING/MONITORING AGENCY NAME(S) AND ADDRESS(ES)
NAWC-PAX
Sung Choi
48066 Show Road, Building 2188, Floor 2
Patuxent River, MD 20670

10. SPONSOR/MONITOR'S ACRONYM(S)
NAWC-PAX

11. SPONSORING/MONITORING AGENCY REPORT NUMBER
N00421

12. DISTRIBUTION AVAILABILITY STATEMENT
No Ristrictions

13. SUPPLEMENTARY NOTES

14. ABSTRACT
The Phase I deliverable is a physic-based model which represents a CMC gas turbine component concomitantly at the material level and the structural level. CMCs are currently being considered and used for aeroengine applications with a goal of increased specific power. A ceramic material must display sufficient capability to withstand the degrading effects that arise from external events such as FOD impacts. In addition to withstanding impact events, the CMC must be able to resist crack propagation through the thickness resulting from FOD induced surface flaws. Further issues of concern: 1) the possibility of impacting materials scratching off the environmental barrier coating (EBC) coating and the subsequent consequences. 2) Given constant environmental attack of a CMC combustor liner due to the vaporization of salty air/water, the rate and sizes of EBC debris that loosen and then impact on turbine nozzle guide vanes. The delivered phase I tool provides the means to cost effectively investigate and resolve these issues in a phase II effort.

15. SUBJECT TERMS
Foreign object damage (FOD); ceramic matrix composites (CMCs); impact; ballistic impact; FOD modeling; impact mechanics; turbo-machinery

16. SECURITY CLASSIFICATION OF: a. REPORT	b. ABSTRACT	c. THIS PAGE	17. LIMITATION OF ABSTRACT	18. NUMBER OF PAGES	19a. NAME OF RESPONSIBLE PERSON
UU	UU	UU	UU		Vinod K. Nagpal
					19b. TELEPONE NUMBER ***(Include area code)*** 440-845-7020

Table of Contents

1.0 Project objectives:

An important part of the design process for turbomachinery components in aeroengine applications is ensuring that the component is resistant to failure from foreign object damage (FOD). This can be accomplished in a cost-effective manner by using physics-based models in conjunction with experimental tests. This concept is known as Integrated Computational Material Science and Engineering (ICMSE). The results from analytic models are used to guide the design of a test matrix and thus reduce the cost of the experimental tests. The experimental tests are used to validate the models or conversely demonstrate where and how the physical theory needs to be redeveloped.

Experimental testing can be expensive and time consuming. Conversely, the development of models and running of simulations can be conducted in a matter of days at a small fraction of the cost of the experiments. The development of a sound design requires agreement between the theoretical models and the experimental data. A design process that utilizes experimental, theoretical and computational tools in this manner is the only practical way CMC material systems can be developed and used in high performance applications in a cost-effective, safe and reliable manner.

The objective of phase I was to develop and demonstrate an initial methodology for analyzing the effects of foreign object damage (FOD) on aeroengine components utilizing CMC materials. The methodology integrates the effects of material behavior into the structural design process. The long term objective is to incorporate this analysis capability into a practical engineering tool for ICSME to develop, design and manufacture the components for tomorrow's high performance vehicles. This methodology is an enabling technology to retain a national technical capability in aerospace engineering.

2.0 Project approach:

The primary reasons why ceramics have not been widely adopted in aeroengine applications are: (a) limitations in their reliability within the harsh gas turbine environment, (b) interfacing ceramic components with adjacent metallic components leads to a mismatch of material properties, and (c) the current high cost of manufacturing components. New ICMSE tools are required to overcome these obstacles. A key element of this particular ICMSE activity is the analysis methodology used to model the FOD and its impact on component reliability. Thus the phase I effort is focused on demonstrating an initial capability to model FOD and the subsequent crack and fatigue behaviors in CMC components. The first step in developing this methodology was to review the literature on FOD to identify the key physical phenomenon present in FOD scenarios. The objective was to ensure that the mechanisms, which need to be engineered in order to ensure a FOD resistant material, are properly modeled. The approach that was used in phase I was to develop physics-based models of the identified constituent material and fiber architectural behavior and attempt to predict the damage map of CMC materials. The results were then compared to available experimental data to evaluate the effectiveness of the new models and their potential for further development into an ICMSE tool.

Figure 1 shows the framework for an ICMSE analysis tool that can be used for evaluating FOD. This methodology can be used to derive a potentially optimal CMC materials architecture. Which will allow a design engineer evaluate a large design space in a cost effective manner.

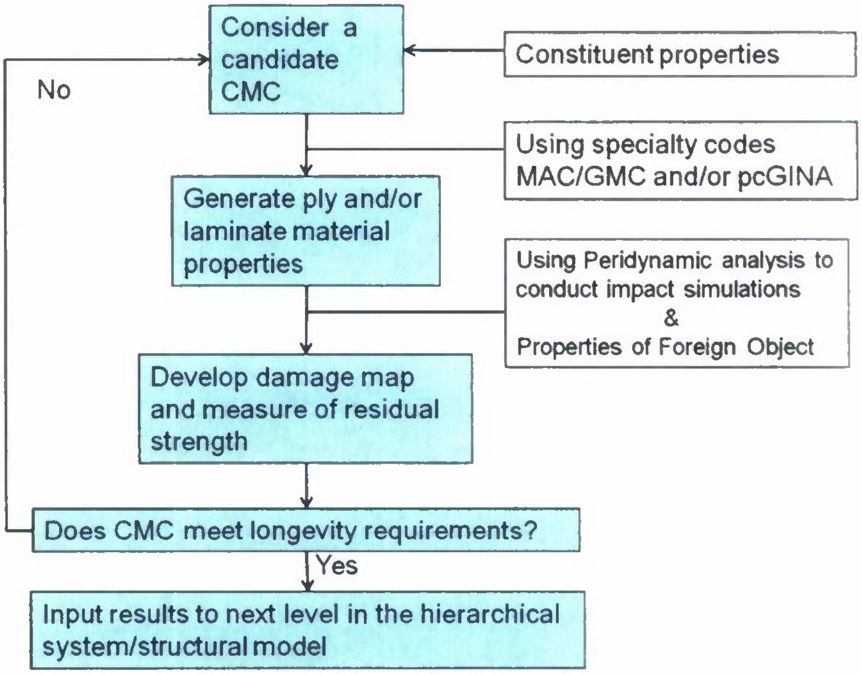

Figure 1: Framework of analysis codes and models. Starting with the models that generate the laminate properties and completing with the models which mimic the physical FOD experiments

The design process must define the internal structure or material architecture for the CMC component that will best meet the structural constraints. This requires that the physics-based predictive tools being developed can accurately predict material behavior and the failure modes due to FOD in composite structures. However to date, no model exists to describe FOD phenomena due to impact dynamics in CMC structures. This can be attributed to the complex nature of impact dynamics coupled with the materials architectural/constituent complications. Accurate prediction of crack behavior includes crack initiation and propagation for both single and multiple cracks. This is challenging in a monolithic material alone, and many approaches to modeling these phenomena require prior knowledge of crack geometry and propagation. This requires additional experimental testing to acquire this knowledge, where a truly predictive capability could avoid this step. In a composite structure the situation is complicated due to the potential for numerous interfaces between fibers, fiber coatings, and lamina. Each can have different material properties and interactions. Key failure modes that must be resolved in a composite structural analysis include delamination, fiber/matrix debonding, fiber breakage, and matrix cracking.

The Peridynamic (PD) methodology [Sillings 2000] was evaluated as the basic methodology for the impact simulation due to its unique capabilities to meet the requirements listed above. Two existing computer codes were investigated to provide PD with laminate material properties: pcGINA and MAC/GMC. The integration of these 3 tools (PD, pcGINA, MAC/GMC) provides the complete framework to conduct the analysis as described above.

3.0 Work completed:

3.1.0 Identification of key physical phenomenon:

An investigation of FOD literature has been conducted to identify the key physical phenomenon present in FOD scenarios. The objective is to ensure that the mechanisms, which need to be engineered in order to ensure a FOD resistant material, are properly modeled. Thus the developed methodology and physic-based models need the capability to represent these physical behaviors.

One caveat is in order: while much engineering can be conducted on a structural level to meet the life constraints of the material, the focus of this work is to develop the tools which will facilitate the tailoring of the material system to be universally applicable.

To engineer FOD resistant materials, one needs models which are able to simulate the proper damage map and to assess the residual strength of the material. To accomplish this task the models need to properly represent crack formation and growth. Proper control of the fiber/matrix interface characteristic is the key to understanding crack propagation and thus obtaining a tough ceramic composite.

3.1.1 Conical damage profile:

In [Choi 2008] and related papers, FOD was experimentally investigated. Two support conditions were considered: first, where the target material was fully support and secondly, where the target material was only partial supported. Furthermore, tests were conducted at both an ambient temperature and at an elevated temperature 1316 C. In addition, a range of materials with differing hardness were considered for the impacting object, some were deformable and others were brittle.

Figure 2 shows the details of the damage resulting from the impact of a projectile on a CMC material sample. There is damage in the form of a crater at the impact site. This damage is due to the breakage of matrix and fiber tows. Furthermore, cracks with cone morphologies form, which emanate at approximate 120^{o} from the impact crater. Delamination is present and spallation of material from the backside occurred in the partial supported test cases.

Figure 3 shows an idealization of the damage progression for the various test cases considered in [Choi 2008]. The PD results demonstrate these patterns very well.

[Choi 2008] concluded that: impact damage increases with impact velocity and that impact damage is a function of impactor hardness. There is spallation of material in the partial support cases due to an additional tensile load in the backside region. Lastly, delamination is clearly evident in both support cases.

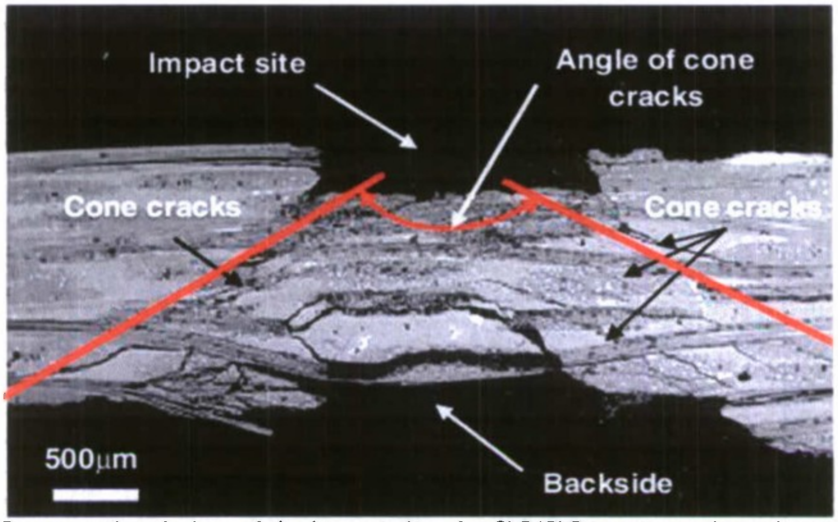

Figure 2: Cross-sectional view of the impact site of a SiC/SiC target specimen impacted at 400 m/s by 1.59-mm steel ball projectile at ambient temperature. Reprinted from [Choi 2008]

[Ogi et al 2010] conducted similar FOD experiments, but they also considered a CMC with a 3D architecture. They conclude that tensile stress during impact was transferred to the z-yarns in the 3D-CMC, which constrain delamination.

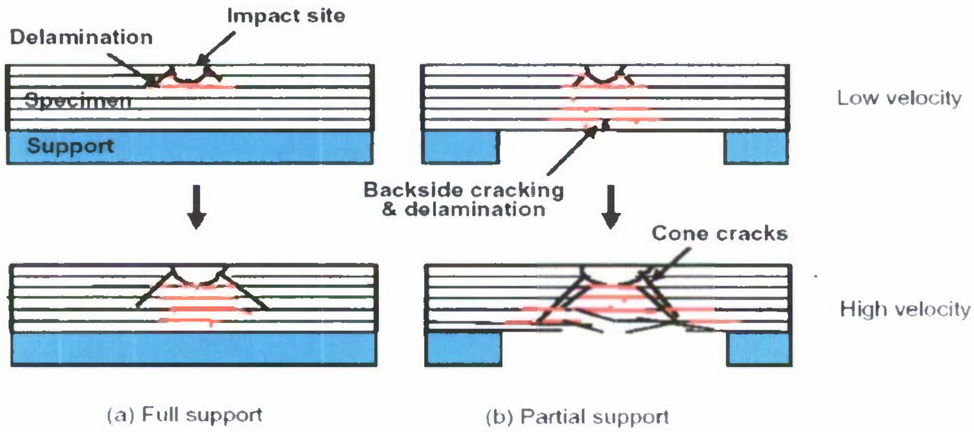

Figure 3: Schematics of damage progress from low (top) to high (bottom) impact velocities in (a) full support and (b) partial support. The vertical arrows indicate a case of increase in impact velocity. Reprinted from [Choi 2008]

3.1.2 Mechanisms of fracture toughness:

In metals, plastic deformations occur around a crack tip, which allows for some strain energy dissipation. Conversely, monolithic ceramics have brittle failure patterns. Thus reinforcement fibers are included to introduce mechanisms for the dissipation of energy.

For CMCs, the local response of the fiber and matrix interface is critical for determining the fracture mechanics. If there is a strong bond between a fiber and the matrix, then a crack propagating through the matrix has a bridge or access point into the fiber. This permits the fiber to be readily cleaved or cut without affecting the dynamics of the crack growth, resulting in a loss of load carrying capability. Conversely, if this interface bond is weak, then the propagating crack might cause the interface to break and the fiber and matrix to debond. This allows for several energy-dissipation phenomena to occur: the crack may be deflected by the fiber and begin to run perpendicular to its original path. If the crack does not change direction, then it will go around the fiber and the fiber will begin to bridge the crack gap. Depending on the nature of the crack patterns a fiber may debond from the matrix material at several points along its length. This will lead to a situation where there is frictional sliding of fiber along the matrix material. As this structured cracking of the matrix material occurs, the fibers will continue to carry increased loads. This will lead to fiber cuts. However, in this case the amount of force required to break the fibers will be greater than if the fiber had been cleaved due a strong bond with the matrix. After a fiber cut has occurred, then it is possible for the fibers to pull out of matrix. As this phenomena occurs, one will also see frictional shear stresses develop at the interface.

3.1.3 Impact resistance of EBC coated SiC/SiC composites

The phase one analysis did not explicitly model the interaction between the environment barrier coating (EBC) and the CMC substrate material. These interactions will be considered in a phase 2 analysis. The EBC coating, figure 4, consists of three sub layers: first a bond coat layer of silicon is deposited on top of the substrate followed by an intermediate mixed layer of mullite + barium strontium aluminum silicate (BSAS), and then there is a top layer of BSAS.

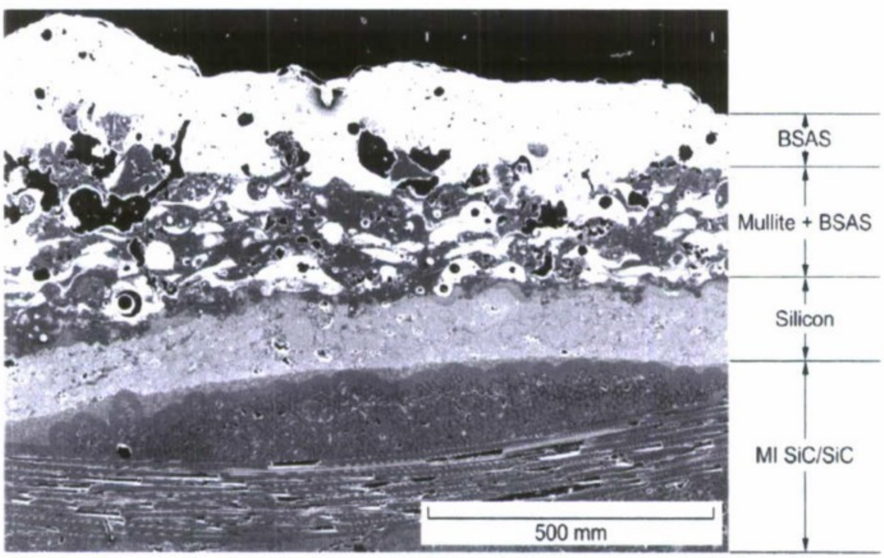

Figure 4: SEM micrograph of typical cross section of plasma sprayed EBC coating on MI SiC/SiC substrate showing microstructure, composition and thickness of EBC sub-layers. Reprinted from [Bhatt et al 2008]

It is critical to raise this point since CMCs require reliable EBC coatings to operate at temperatures greater than 1100 °C. Without an EBC coating the substrate material does not have adequate life [Bhatt et al 2008]. The weakest link in the (EBC) is the interface between the intermediate coat (a mixture of mullite and BSAS) and the silicon bond coating. Any cracking or scratching off of the EBC provides an access point for hostile environmental attack to the CMC material. It is worth exploring if a coating can be used to increase the duration of impact or to reduce impact based stresses.

3.2.0 Material selection

The material chosen for analysis is a melt-infiltrated silicon carbide fiber/silicon carbide matrix composite N24A MI SiC/SiC, figure 5. The composite used in this study has eight plies for a minimum thickness of .08 in.

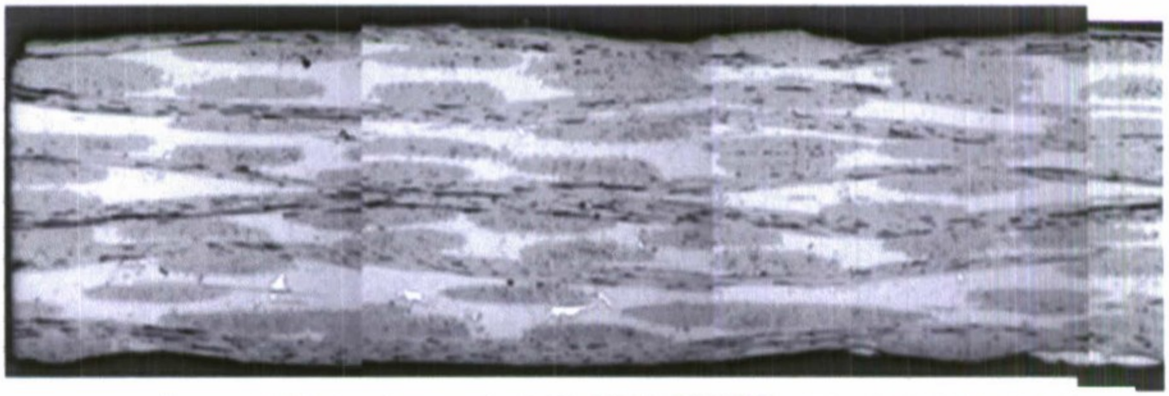

Figure 5: Photomicrograph of N24A MI SiC/SiC composite. [Mital 2009]

The fiber tows are bundles of Sylramic[1] –iBN fiber which are then woven into a five-harness fabric perform, figure 6a, with a layup sequence of $[0^0/90^0]_{4S}$. There are 20 ends per inch (epi). The fiber tow is forged in an elliptical shape with a total thickness of 0.005 in and an aspect ratio of 9:1.

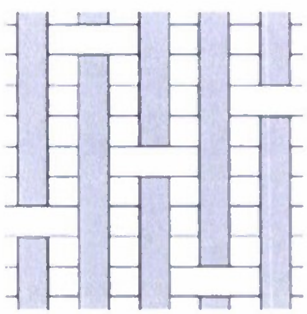

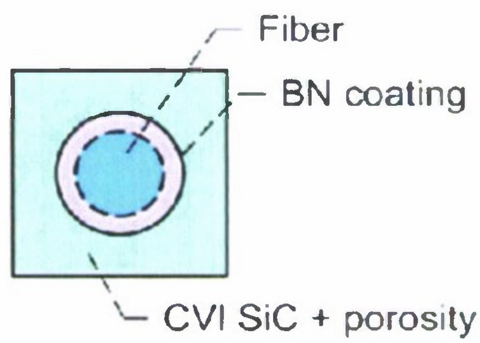

Figure 6: (a) five-harness woven fabric perform, (b) composition of a fiber tow [Mital 2009]

The fiber tow is itself a composite, figure 6b, comprised of bundles of Sylramic[1] –iBN filaments coated with a silicon-doped boron nitride (BN) interface. The preform is then impregnated with a SiC matrix via a chemical vapor infiltration (CVI) process to complete the rigid perform mat. These tows can be seen in Figure 5 as the dark grey material. The preform, Figure 6a, is then filled with a SiC matrix utilizing a slurry-casting melt infiltration process, which is visible in figure 5 as the light grey material. The analysis tool may be used to model other material systems.

3.3.0 Components of methodology/tool

This methodology/tool uses preexisting specialty software packages which have been extensively used by NASA and private industry. Application of this methodology has been demonstrated on the CMC of high interest. First the tow properties are determined from the properties of its constituents using MAC/GMC. Then the laminate properties are generated using pcGINA or MAC/GMC depending on the users' preference. Finally, the material properties generated from pcGINA or MAC/GMC input into the Peridynamics model and the impact simulation is conducted; which generates a damage map and an estimate for residual strength.

3.3.1 Peridynamic theory

Despite the development of many important concepts to predict material behavior and failure, the prediction of failure modes and residual strength of composite materials is a challenge within the framework of the finite element method (FEM). Furthermore, the previous methods cannot address the nucleation of damage in a continuous material. The field of fracture mechanics is primarily concerned with the evolution of pre-existing defects within a body, rather than the nucleation of new defects. Even when addressing crack growth, the FEM suffers from the inherent limitation that it requires remeshing after each incremental crack growth. In addition to the need to remesh, existing methods for fracture modeling also suffer from the requirement of an external crack growth criterion. This criterion prescribes how damage evolves a priori based on local conditions, and guides the analysis as to when and how damage initiates and propagates. Considering the difficulty in obtaining and generalizing experimental fracture data, providing such a criterion for damage growth, especially in composite structures, clearly presents a major obstacle to fracture modeling using conventional methods. This prevents such methods from being applicable to problems in which multiple damage growth occurs and interacts in complex patterns.

The governing equations of the FEM are based on the partial differential equations (PDEs) of classical continuum mechanics and that the spatial derivatives required by the PDEs do not, by definition, exist at crack tips or along crack surfaces. Therefore, the basic mathematical structure of the formulation breaks down whenever a crack appears in a body. Various special techniques have been developed in fracture mechanics to deal with this limitation. Generally, these techniques involve redefining a body in such a way as to exclude the crack, then applying conditions at the crack surfaces as boundary conditions.

In order to overcome these problems, [Silling 2000] introduced a nonlocal theory that does not require spatial derivatives—the peridynamic (PD) theory. The main difference between the PD theory and classical continuum mechanics is that the former is formulated using integral equations as opposed to derivatives of the displacement components. This feature allows damage initiation and propagation at multiple sites, with arbitrary paths inside the material, without resorting to special crack growth criteria. In the PD theory, internal forces are expressed through nonlocal interactions between the material points within a continuous body, and damage is a part of the constitutive model. Interfaces between dissimilar materials have their own properties and damage can propagate when and where it is energetically favorable for it to do so.

With the PD theory, damage in the material is simulated in a much more realistic manner compared to the classical continuum-based methods. The broken interactions may align themselves along surfaces that form cracks and the deformation is discontinuous across such as a crack, yet the integral equations continue to remain valid. The PD theory has been utilized successfully for damage prediction in many problems.

In a peridynamic simulation, the distances between points in the material are monitored and stretches between these points are determined. When the stretch between a pair of points exceeds the specified failure stretch, the peridynamic bond between these material points is broken. Hence, these material points will no longer interact and failure takes place. Material failure is therefore intrinsic to the theory, and there is no need for any complex treatment to capture crack initiation and propagation. Thus, damage is simulated in a much more realistic manner compared to classical continuum-based methods.

In the case of an isotropic material where there is no directional dependence of the interactions between the material points. However, if anisotropic materials such as a fiber-reinforced composite structure are considered, the directional dependency must be included in the peridynamic analysis. Therefore, four different peridynamic material parameters are introduced, as shown in figure 7, to model a fiber-reinforced composite laminate. A material point of interest can only interact with a material point located either in the same ply or in the adjacent plies.

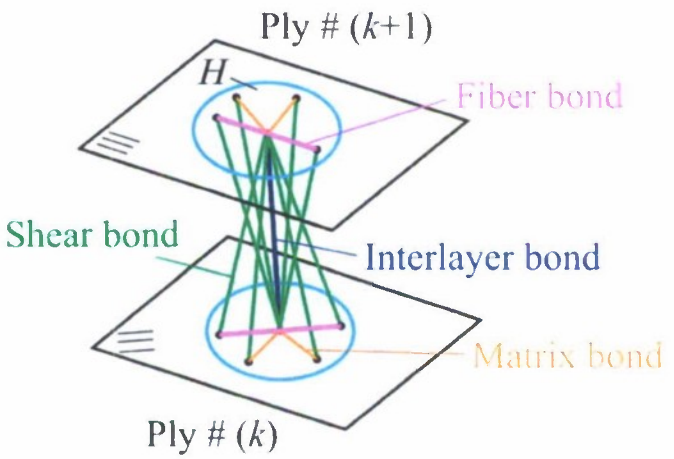

Figure 7: Peridynamic bonds for a fiber-reinforced composite laminate

3.3.2 MAC/GMC

MAC/GMC is a software package for the analysis of composite material and laminates developed at the NASA Glenn Research Center. It is based on the generalized method of cells (GMC) micromechanics theory [Paley and Aboudi, 1992]. It calculates the local stress and strain fields generated in the composite material given spatially varying constituents. With this software package one may assess the inelastic material behavior and various type of damage to a laminate given inhomogeneous local models of the materials constituents. The set of tools encoded in MAC/GMC has several advantages over the commonly used finite element micromechanics approaches. MAC/GMC provides several constitutive models for heterogeneous materials. This software package allows one to represent the composite as continuum without any boundaries. Thus material models generated in MAC/GMC can be seamlessly embedded within higher scale structural analyses, such as finite element. The MAC/GMC model is designed to represent the composite behavior at a material point.

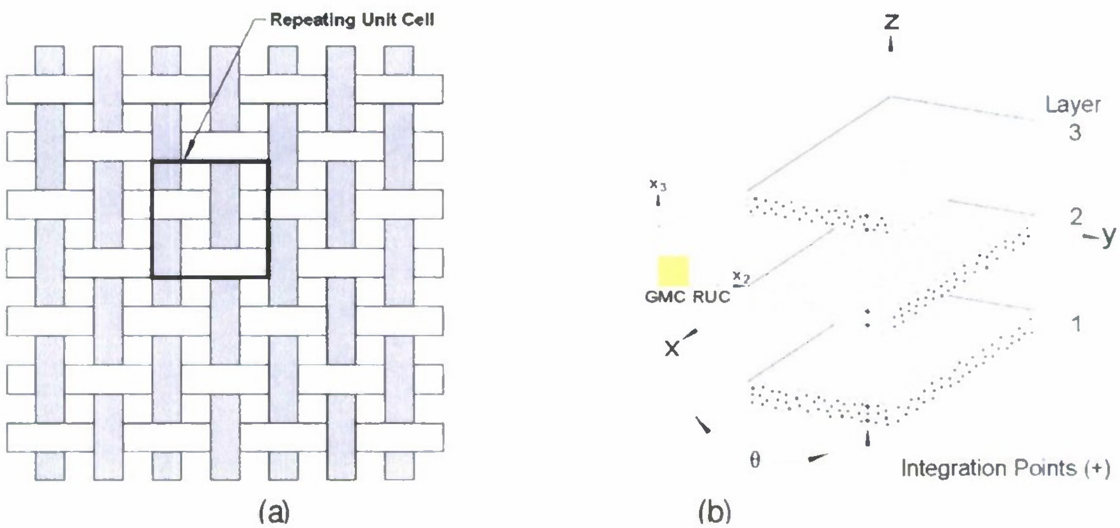

Figure 8: a) Defining a Repeating Unit Cell (RUC) ; b) Geometry employed in MAC/GMC for laminate theory analysis. Reprinted from [Bednarcyk 2002]

With the repeating unit cell (RUC) method, one identifies a pattern which repeats throughout the material. In the doubly periodic (RUC) method, as depicted above, the unit cell repeats in a plane, whereas, with the triple periodic RUC method the unit cell repeats in three dimensions. There may be more than one distinct repeating unit cell in the material. The (RUC) is not meant to model a laminate, but instead it considers an idealized composite in an infinite plane or space. Thus when using the RUC method in the MAC/GMC code, one is not concerned with thicknesses, heights and widths.

Inside the RUC of figure 8a), one can see tows in both the fill and warp directions as well as space where the matrix material is otherwise present. Thus, the RUC is further divided into sub cells, such that there is to be only one type of material per sub cell. The micromechanics equations are then applied and solved for each sub cell within the RUC.

In addition one may use MAC/GMC to generate the material response of a ply or laminate via classical lamination theory, figure 8b). The input for the laminate solver is very similar to the input for the RUC method. The main difference being, that the user must supply information regarding the orientations of the fibers, thicknesses and number of plies which comprise the laminate plate.

Previous work has shown that the traditional one step three-dimensional homogenization procedure for modeling woven composites is inaccurate due to a lack of shear coupling in the model. This initial shortcoming has been resolved by the introduction of the two step homogenization procedure. Wherein, each RUC identified, is first homogenized through its thickness before being re-assembled with the other RUCs anisotropic D matrices and then all are homogenized across the plane.

(a) (b)

Figure 9: a) a plain weave composite b) the exploded view of that plain weave composite reprinted from [Bednarcyk 2000]

Figure 9 a), is a MAC/GMC model of a plain weave CMC, figure 9 b) is an exploded view of the same model. Imagine dividing the material into serial cross-sections and separating it as in figure9 b). Closer inspection of figure 9b) allows one to identify six basic groups which can be seen in figure 10 a). A first-step model is developed for each group, and once MAC/GMC has derived the full anisotropic D matrix for each of the six groups then one uses that information as input into the second-step model, which can be seen in figure 10b)

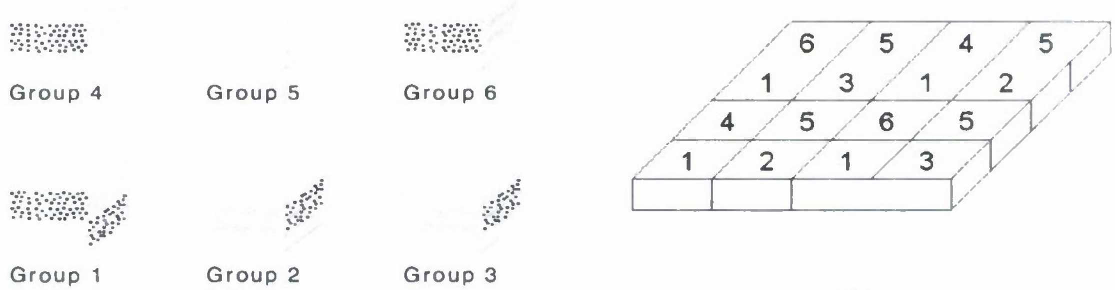

(a) (b)

Figure 10: a) six distinct material groups for the composite b) the reassembly of the groups in 10a) reprinted from [Bednarcyk 2000]

3.3.3 pcGINA

pcGINA stands for " PC based Graphical Integrated Numerical Analysis program". It is used for designing and predicting the properties of textile reinforced composites. It predicts the static elastic and thermal properties of textile composites. It was selected for use in this work due to the fact that it is widely known in industry. As its use is a good fall-back position and double check of the GMC/MAC models.

However, it was developed for Polymer Matrix composites (PMC) not CMCs. It is not a micro-mechanics code like GMC/MAC rather it is a fiber weave, or textile code. Thus, there are a few times when the user has to "trick" the user input screens; as a PMC does not have the extra step of a CVI infiltration of the yarn to create a tow. Some DOD-AF [Gowayed et al 2007] work has adapted pcGINA to work with CMC materials, however the authors are not aware of the full extent. None-the-less, it clearly belongs in a suite of codes along-side GMC/MAC, for verification and validation purposes.

3.4.0 Models

First to be described is the MAC/GMC model used to determine the tow properties. Then the models used to determine the laminate material properties presented. Lastly, the impact models are described.

3.4.1 Tow model

Unlike a polymer matrix composite (PMC), one must derive the material properties of the tow before one may derive the material properties of a ply or laminate panel. Since, the tow is comprised of filaments, possibly braided into a yarn, which are coated by a boron nitride (BN) interface material before being infiltrated with a silicon carbide (SiC) matrix material. The tow itself should be thought of as a unidirectional lamina. So a clear distinction must be maintained between the ratio of filaments to chemical vapor infiltrated (CVI) matrix material within the tow, and the ratio of tows to melt infiltrated matrix material in the ply or laminate.

$$\text{Filament volume fraction within the tow} = \frac{(\text{number of filaments}) * (\text{area of a filament})}{\text{area of tow}} \qquad 1)$$

Even though one should think of the CMC tow as a unidirectional lamina, in reality it may not be, since the filaments may be braided into a yarn. If this happens to be the physical situation MAC/GMC has models in its standard library which can represent a braided yarn structure. Figure 11 (b) is the MAC/GMC model used to describe the idealization of the tow as depicted in figure 11(a). One uses equation 1 to determine the filament volume fraction within the tow.

<u>The input deck for the tow model, figure 11b:</u>

Number of materials:	3
Constitutive models:	Elastic
Materials:	iBN-Sylramic
	CVI-Sic
	CVI-BN

Analysis type: (*RUC) Repeating Unit Cell Analysis
Analysis model: Doubly periodic GMC
RUC architecture: 7x7 Circular Fiber Approx., Rectangular Pack
Fiber volume fraction: 0.5
Ratio of interface
thickness to fiber radius: 0.124

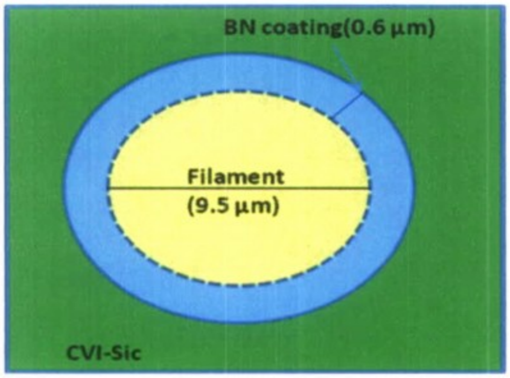

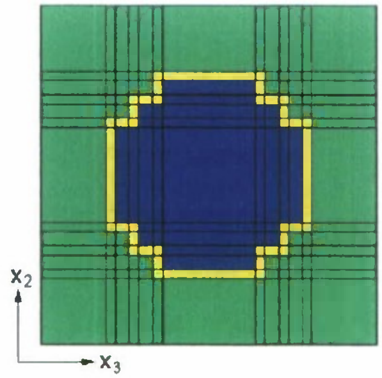

a) b)

Figure 11: a) idealized model of a tow, b) MAC/GMC model of the idealized tow

Table 1: Input values to the tow model, constituent properties

	E_A (GPa)	E_T (GPa)	ν_A	ν_T	G_A (GPa)	α 10^{-6} K
Material properties at room temperature						
Sylramic fiber	380	380	0.17	0.17	162.4	4.6
CIV-SiC matrix	380	380	0.17	0.17	162.4	4.6
BN coating	21	21	0.22	0.22	8.607	5.2
Material properties at high temperature (1204 C)						
Sylramic fiber	365	365	0.17	0.17	156	8.0
CVI-SiC matrix	358	358	0.17	0.17	153	9.0
BN coating	14	14	0.22	0.22	5.738	10.0

Table 1 lists the input values for this tow model, figure 11b). E_A is Young's modulus in the axial direction while E_T is Young's modulus in the transverse direction. Similarly, ν_A Poisson's ratio in the axial direction and ν_T is Poisson's ratio along the transverse direction. G_A is the shear modulus in the xy plane. α is the coefficient of thermal expansion.

3.4.2 pcGINA laminate model

If the laminate is balanced, then the material properties of the ply are the same as the material properties of the laminate, with the exception of the effect of thickness.

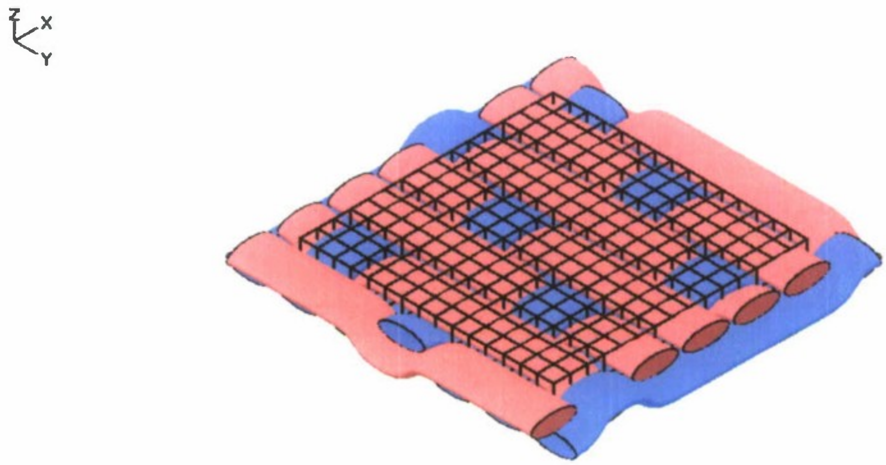

Figure 12: pcGINA model of a 5-harness satin weave composite

In figure 12, for both the red and blue tows, it is assumed that the major axis is 45 milli-inches (mil) and that the minor axis is 5 (mil). The tow initially starts with a cylindrical geometry, but ends up with an ellipsoidal shape due to fabrication. The angle between the tows is 90^o. This leads to a total fiber volume fraction of 0.70911, of which 0.35455 is the blue tows, and the other 0.35455 is the red tows. In this context, fiber does not refer to the filaments which comprise the tows, instead the term fiber refers to the tow. Table 2 lists the input values used in the pcGINA ply model depicted in Figure 12.

Table 2: input material properties

	E_A (GPa)	E_T (GPa)	ν_A	ν_T	G_A (GPa)	α_A 10^{-6} K	α_T 10^{-6} K
Material properties at room temperature							
Tow fiber	320	149	0.176	0.15	59.6	4.6	4.7
MI-SiC matrix	310	310	0.17	0.17	132.48	4.7	4.7
Material properties at high temperature (1204 C)							
Tow fiber	306	120	0.175	0.137	47.6	8.5	8.8
MI-SiC matrix	276	276	0.17	0.17	117.95	9	9

The version of pcGINA used in this study, v.11.98, is designed to model PMCs as opposed to CMCs. Therefore, certain manipulations are required: after inputting values for the filaments, pcGINA provides a screen to input yarn specific parameters. The values inputted on the yarn screen are required by pcGINA, however their engineering value has been made redundant by the tow model. It is important, that the values on this screen be inputted in such a way that the filament packing factor, generated by pcGINA, is calculated as 1. The program will issue a warning, but this is to be ignored. Recall that the tow's properties were calculated prior to the use of pcGINA.

3.4.3 MAC/GMC laminate model

MAC/GMC was used to analyze the woven reinforcement architecture of the N24A CMC. Both the one-step and two-step homogenization procedures from [Mital et al 2009] have been reproduced. The two step procedure was implemented since the single-step procedure has been shown to derive less than accurate results for woven composites. Conversely, for unidirectional composites the one-step homogenization procedure provides accurate results. Table 2, above, lists the material properties used in these models. MAC/GMC internal constitutive models allow specification of an arbitrary direction of traverse isotropy. Material 5 is the melt infiltrated SiC matrix. Materials 1-4 and 6-7 are all the fiber tow and thus have the same material properties. The difference between them is a vector which defines their direction of traverse isotropy.

<u>The input deck for the woven CMC model, figure 14:</u>

Number of materials:	7 (NMATS=7)
Constitutive models:	Arbitrary transversely isotropic (CMOD=9)
	Elastic (CMOD=6)
Materials:	User-defined (MATID=U)
Material property source:	Read from input file (MATDB=1)
Material properties:	See table 2 above
Direction of trans. Isotropy:	
	Material #1: (0, 0, 1)
	Material #2: (0, 1, 0)
	Material #3: (2.5, 14, 0)
	Material #4: (-2.5, 14, 0)
	Material #6: (2.5, 0, 14)
	Material #7: (-2.5, 0, 14)
Analysis type:	(*RUC) Repeating Unit Cell Analysis
Analysis model:	Triply periodic GMC (MOD=3)
RUC architecture:	User-defined (ARCHID=99)
No. sub-cells in x1-dir.:	4 (NA=4)
No. sub-cells in x2-dir.:	10 (NB=4)
No. sub-cells in x3-dir.:	10 (NG=10)
Sub-cell depths:	2.5, 2.5, 2.5, 2.5 (D=2.5, 2.5, 2.5, 2.5)
Sub-cell heights:	36.0,14.0,36.0,14.0,36.0,14.0,36.0,14.0,36.0,14.0
Sub-cell lengths:	36.0,14.0,36.0,14.0,36.0,14.0,36.0,14.0,36.0,14.0

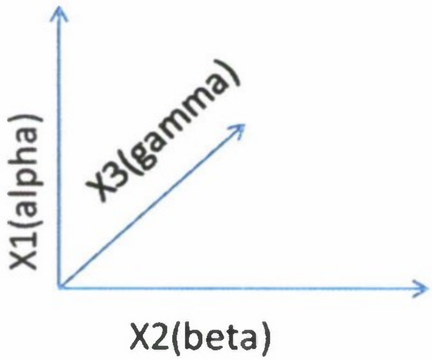

a)

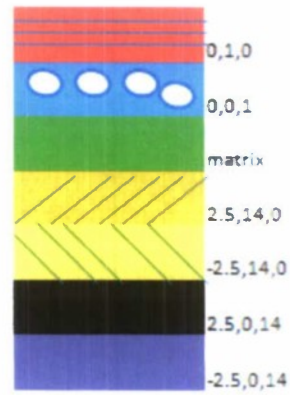

b)

Figure 13: a) material coordinate system b) legend for fiber orientation

Figures 13a) and 13b) are the material coordinate system and the legend for the fiber orientation of figure 14. The vector coordinates listed in the legend 13b) are defined by the coordinate system depicted in figure 13a). The fibers where not draw on the black and purple cells; as these lines would have to be drawn through the thickness of the page. The green cells represent the melt infiltrated matrix material. The red, orange and yellow cells represent the tows in the x2 direction, whereas the blue, black and purple cells are the tows in the x3 direction. Inspection of gamma one in figure 14, starting at the leftmost column in the x2 direction, shows the red tow at the bottom two rows. As one moves in the x2 direction, the red tow stays in the bottom two rows, until the sixth column is reached, at which point the red fiber tow begins to rise, depicted as the orange cells, and then in the seventh column the red fiber tow is on the topmost two cells in the x1 direction. In the eighth column along the x2 direction, the red fiber tow begins to drop down in the x1 direction, which is depicted as the yellow cells. Finally the red tow is once again on the bottom most rows for columns nine and ten. The same behavior can be seen for the blue, black and purple tow. However, instead of staying on one gamma cross-sectional slice, the weaving behavior of the blue tow will be seen by traversing from gamma one to gamma five. Consider gamma one, column three, the top two rows, in this location is the blue tow. Now, in gamma two, the blue tow is depicted as purple cells as it drops down in the x1 direction. Then in gamma three, the blue tow occupies the two bottommost cells in the x1 direction. In gamma four, the blue tow rises through the x1 direction and this is depicted by the black cells. Finally, in gamma five, the blue tow has returned to the topmost cells in the x1 direction.

Thus one may build a MAC/GMC model represent any custom material architecture. The input deck has commands to define each material of interest. One then has a set of commands to define how the unit cells are connected and which material they represent. Finally, one has control over the dimensions of each unit cell. Recall, that the MAC/GMC model represents a material point which is callable by a structural model. Embedded in MAC/CMC is a library of material constitutive behavior models. This eliminates, in many cases, the need to write custom subroutines.

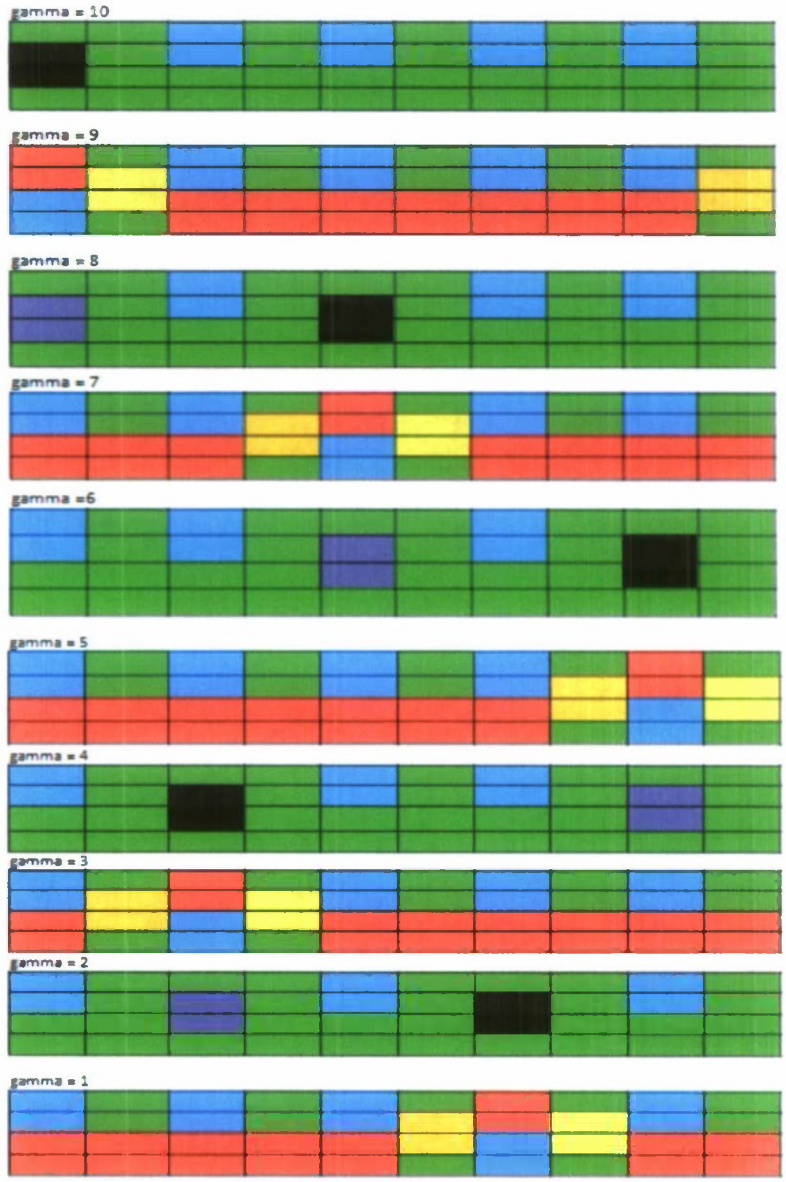

Figure 12: MAC/GMC model of a 5 harness satin weave CMC

3.4.4 PD model for a FOD event:
A SiC/SiC ceramic matrix composite (CMC) is impacted either by a rigid or a deformable (steel) indenter as shown in figure 13. Two different boundary conditions are considered, i.e. full support and partial support.

The geometrical properties of the SiC/SiC CMC is specified as $L = 45\text{mm}$, $W = 8\text{mm}$, $H = 2.25\text{mm}$. The spherical impactor has a diameter of $D = 1.5\text{mm}$. For the partial support case, the distance between two supports is specified as $B = 20\text{mm}$.

The SiC/SiC CMC material is assumed to be isotropic with an elastic modulus of $E = 220\text{GPa}$ and density of $\rho = 2400\text{kg/m}^3$. The elastic modulus and density of the steel impactor are $E = 200\text{GPa}$ and $\rho = 7860\text{kg/m}^3$, respectively. The steel impactor can exhibit plastic deformation when it experiences stress state near the ultimate strength of the material which is specified as 2.0 GPa. The SiC/SiC CMC and steel impactor have fracture toughness values of $K_I = 25.\text{MPa}\sqrt{m}$ and $K_I = 90\text{MPa}\sqrt{m}$, respectively.

(a) (b)

Figure 13: SiC/SiC CMC is impacted by a rigid indenter (a) Full support (b) Partial support

Two different impactor velocity conditions, $v_0 = 200\text{m/s}$ and $v_0 = 400\text{m/s}$ are considered for both full and partial support cases.

Peridynamic model is generated by using 51976 material points with grid size and horizon values of $\Delta x = 0.25\text{mm}$ and $\delta = 0.75375\text{mm}$, respectively. The bond constants for the CMC and steel impactor are $c = 2.6\times10^{12}\text{ N/m}^6$ and $c = 2.37\times10^{12}\text{ N/m}^6$, respectively. The critical stretch values of CMC and steel impactor are specified as $s_0 = 0.00276$ and $s_0 = 0.0157$, respectively, which can be computed by using the relations derived by Silling and Askari [8],

$$s_0 = \sqrt{\frac{4K_I^2}{9E^2\delta}} \text{ for 2-D CMC plate and } s_0 = \sqrt{\frac{2.5K_I^2}{3E^2\delta}} \text{ for 3-D steel impactor}$$

Stable time step size used in the dynamic analysis is chosen as $\Delta t = 1.3\times10^{-8}\text{s}$. The displacement boundary conditions are applied to one layer of material points at the bottom edge of the model by constraining all displacement components.

4.0 Results

4.1.0 MAC/GMC tow results

Table 3 lists a comparison between the results of this work and the results published in [Mital et al 2009]. There are slight discrepancies between the two sets of results. However, most of these differences are less than 10 percent. E_A is Young's modulus in the axial direction while E_T is Young's modulus in the transverse direction. Similarly, ν_A Poisson's ratio in the axial direction and ν_T is Poisson's ratio along the transverse direction. G_A is the shear modulus in the xy plane. α is the coefficient of thermal expansion.

Table 3: Comparison of the MAC/GMC tow model results with the published results

E_A (GPa)	E_T (GPa)	ν_A	ν_T	G_A (GPa)	α_A 10^{-6} K	α_T 10^{-6} K
Literature results at room temperature						
320	149	0.176	0.15	59.6	4.6	4.7
This study's results at room temperature						
320.8	150.4	0.1756	0.1507	60.12	4.662	5.328
Literature results at high temperature (1204 C)						
306	120	0.175	0.137	47.6	8.5	8.8
This study's results at high temperature (1204 C)						
304.7	120.5	0.1752	0.1378	47.94	8.409	8.744

4.2.1 pcGINA laminate results

Tables 4 and 5 have a comparison of results from this study and the results published in [Mital et al 2009]. The difference, between the material properties, generated by the two studies are for most case within rounding error. The worst discrepancy is Young's modulus in the z direction for the room temperature case. The two differ by approximately 4.6%.

Table 4: Comparison of room temperature results with the literature

	E_x (GPa)	E_y (GPa)	E_z (GPa)	ν_{xy}	G_A (GPa)
This study	247.604	247.604	182.146	0.1138	103.635
Lit. model	248	248	174	0.11	102
Lit. data	252	252	82	0.13	n/a

Table 5: Comparison of high temperature (1204 C) results with the literature

	E_x (GPa)	E_y (GPa)	E_z (GPa)	ν_{xy}	G_A (GPa)	α 10^{-6} K	kx	kz
This study	221.746	221.746	150.567	0.116	87.82	7.811	17.43	12.66
Lit. model	221	221	151	0.11	86	7.8	18	12
Lit. data	230	230	n/a	n/a	n/a	6	20	18

4.2.2 MAC/GMC laminate results

Tables 6 and 7 compare the results found in this study with the results published in literature [Mital et al 2009].

Table 6: Single-step homogenization procedure

	E_x (GPa)	E_y (GPa)	E_z (GPa)	ν_{xy}	G_A (GPa)
Material properties at room temperature					
This study	232.8	232.9	182.8	0.1243	70.64
Lit. model	233	233	183	0.125	70.7
Lit. data	252	252	82	0.13	n/a
Material properties at high temperature (1204 C)					
This study	202.6	202.7	151.4	0.113	57.33
Lit. model	203	203	151	0.11	57.3
Lit. data	230	230	n/a	n/a	n/a

Table 7: Two-step homogenization procedure

	E_x (GPa)	E_y (GPa)	E_z (GPa)	ν_{xy}	G_A (GPa)
Material properties at room temperature					
This study	252.94	249.01	183.11	0.128	74.11
Lit. model	252	252	183	0.127	74.5
Lit. data	252	252	82	0.13	n/a
Material properties at high temperature (1204 C)					
This study	227.78	223.43	151.60	0.117	60.89
Lit. model	225	225	151	0.12	60.9
Lit. data	230	230	n/a	n/a	n/a

4.3.1 PD results for a rigid impactor

The damage predictions obtained for two different boundary conditions for an impactor velocity of $v_0 = 200\,m/s$ and $v_0 = 400\,m/s$ are depicted in Figures 14 and 15. In figure 15(a), a substantial damage occurs around the impacted region for the full support case. For the partial support case, a conical damage shape is observed and the damage occurs not only at the impacted region but also at the bottom of the specimen. For a higher velocity case, i.e. $v_0 = 400\,m/s$, similar damage shapes are observed with a bigger damage area.

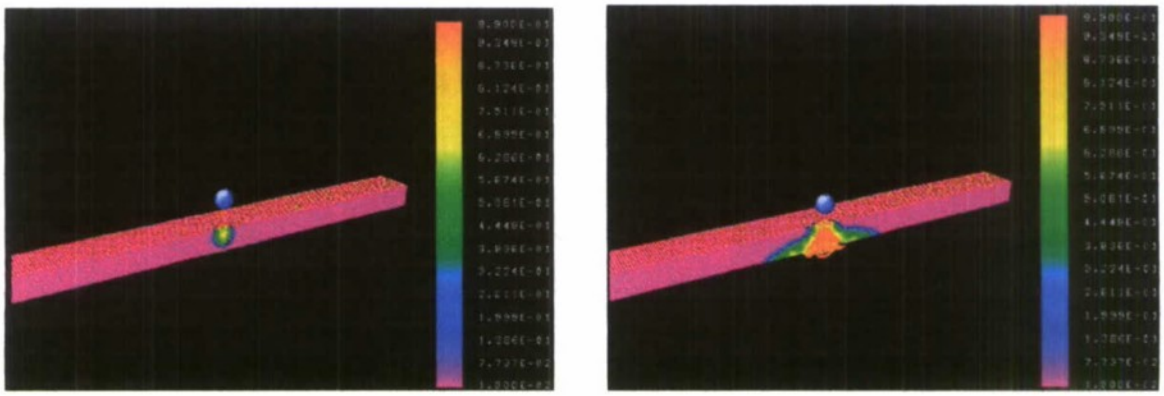

(a) (b)

Figure 14: Damage plot for SiC/SiC CMC impacted by a rigid indenter with a velocity of $v_0 = 200\,m/s$ (a) Full support, (b) partial support

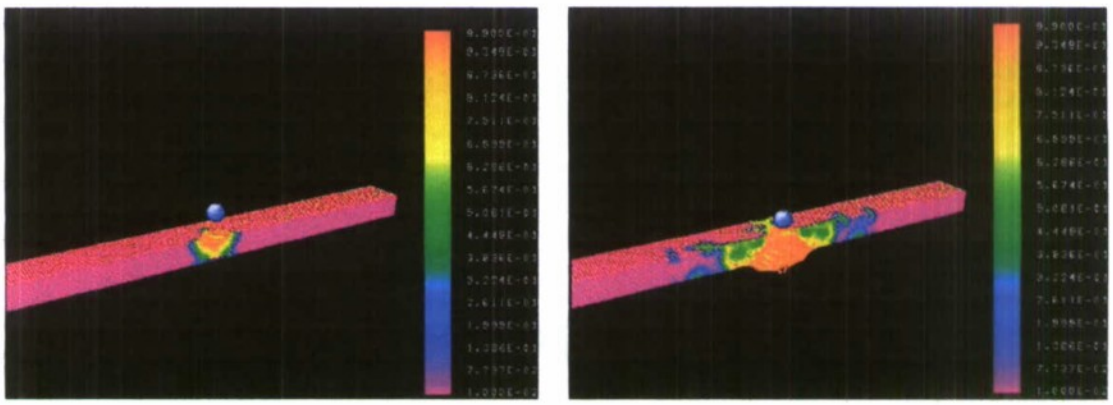

(a) (b)

Figure 15: Damage plot for SiC/SiC CMC impacted by a rigid indenter with a velocity of $v_0 = 400\,m/s$ (a) Full support, (b) partial support

Peridynamic damage prediction can be qualitatively compared against experimental results obtained by [Choi 2008], as shown in Figure 3. The experimental observations and PD simulation results appear to be in close agreement as shown in Figures 14 and 15.

4.3.2 PD results for a deformable (steel) impactor

The damage plots obtained for two different boundary conditions for an impactor velocity of $v_0 = 200 m/s$ and $v_0 = 400 m/s$ are depicted in figures 16 and 17. As shown in figure 16a, substantial damage occurs around the impacted region for the full support case. For the partial support case, in addition to the damage occurrence around the impacted region, a conical damage occurs at the bottom of the specimen as shown in figure 16b. For both cases, the steel impactor is significantly damaged and experiences plastic deformation. For a higher velocity case, i.e. $v_0 = 400 m/s$, shown in figure 17, similar damage patterns are observed with larger damage areas. Also, the steel impactor experiences complete damaged through fragmentation.

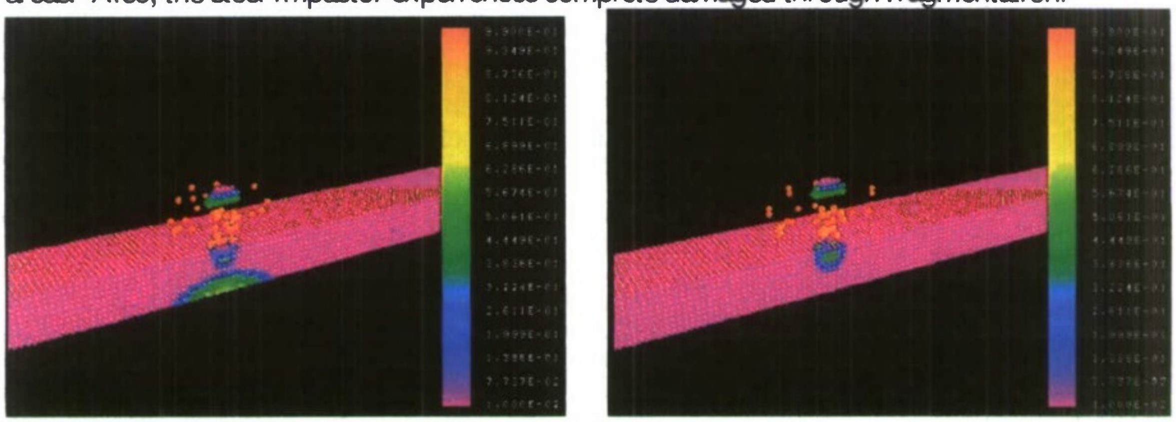

Figure 16: Damage plot for SiC/SiC CMC impacted by a steel impactor with a velocity of $v_0 = 200 m/s$ (a) Full support, (b) partial support

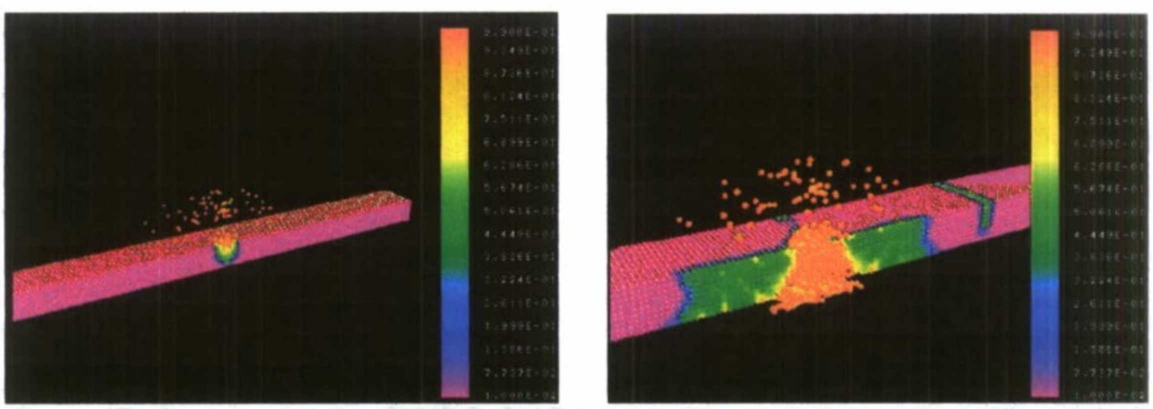

Figure 17. Damage plot for SiC/SiC CMC impacted by a steel impactor with a velocity of $v_0 = 400 m/s$ (a) Full support, (b) partial support

5.0 Conclusions

There is substantial interest in developing CMC material systems for use in turbo-machinery applications. There are definite increases to specific power and/or reductions in fuel consumption when CMCs are incorporated into aeroengine design.

The objective of phase I was to develop and demonstrate an initial methodology for analyzing the effects of foreign object damage (FOD) on aeroengine components utilizing CMC materials.

To engineer FOD resistant materials, one needs models which are able to simulate a proper damage map and to assess the residual strength of the material. To accomplish this task the models need to properly represent crack formation and growth. Proper control of the fiber/matrix interface characteristic is the key to understanding crack propagation and thus obtaining a tough ceramic composite.

This objective has been successfully completed by the development of a proof-of-concept model for one particular CMC material system. The effective material properties of the CMC material system were generated by using MAC/GMC to homogenize the constituent properties. A Peridynamic model was used to simulate the FOD impact, and the results match literature experiments very well.

Peridynamic theory is an evolution of the finite element method. Its main strength over finite elements is that the damage law is embedded into a given model's "mesh". Thereby, allowing damage to occur along the paths which are energetically favorable. Whereas, in the FEA method, one is required to constantly re-mesh the model and have apriority information about the crack path.

The suite of integrated codes demonstrated in this effort offer a cost effective and reliable tool for design. The use of this tool will reduce number of experimental tests required early in the design process for an application built with CMC materials.

The presentation, at the 2010 CMC session of Cocoa Beach, of phase I results generated much interest from potential industrial partners, such as General Electric and Pratt & Whitney RocketDyne.

6.0 Recommendations

While the phase I results are encouraging, further work is required to fully develop and optimize this approach. The next obvious step is to demonstrate the approach using pertinent data obtained from various materials systems together with a range of impact variables.

To ensure commercial relevance we intend to develop a strategic partnership with GE or RocketDyne; which will guarantee that the methodology is applied to aero-engine applications of interest to NAVAIR.

The phase I literature survey indicated: the need to explicitly model the effect that EBC coatings have with respect to FOD; the need to explicitly model the effects of voids, present in the matrix materials.

As this methodology matures there will be a need to increase the coupling of MAC/GMC and PD and prototype the automation of data transfer between the two software packages.

7.0 Short abstract of proposed follow-on research and development
The priority objective is to facilitate the development of CMC material systems for use in turbo-machinery applications. In support of this goal, the obvious step is to analyze an aeroengine component with the phase I methodology. Thus a component of interest will be decomposed into a set of streamlined geometries that are solved piecewise by the phase I tool. A detailed analysis using Peridynamics models of various CMC material systems would be conducted. This requires conducting experimental coupon testing to calibrate the PD impact models to the various material systems of interest. Then the optimal material configuration would be evaluated in an appropriate structural model. This approach ensures that meaningful information is generated as the tool is refined. If the loading spectrum is available then the fatigue life can be estimated using GMC/MAC.

Many of the composite material systems are novel and lack extensive databases. Appropriate design margin can be established by probabilistic structural and sensitivity analyses. These techniques will also quantify the effects of uncertainties and identify influential variables. This will ensure that the material system is insensitive to key design criteria.

These activities will ensure that the requirements for a prototype software process will be specified to control the automation of data flow between software codes.

8.0 Transition plan
We plan to develop a strategic partnership with either GE or RocketDyne to apply the methodology to an aero-engine application of interest to NAVAIR. The phase II work will require a balanced development effort between generating a polished and refined / re-useable analysis tool and applying the current tool to a more complex application of interest to the stakeholders.

Given an application problem of interest, for the industrial partner and NAVAIR, N&R Engineering and UofA would work on both the tool development and an idealized structural model which would be delivered to both the industrial partner and NAVAIR. The industrial partner would be free to customize this model as suits their needs, with N&R Engineering and UofA providing tool support/development as required.

A marketing study will be conducted to evaluate potential interest for this tool in other non-aeroengine applications.

References

Aboudi, Jacob, "Micromechanical Analysis of Thermo-Inelastic Multiphase Short-Fiber Composites", Compos. Eng., vol. 5, no.7, 1995, pp. 839-850

Bednarcyk, Brett A.; Arnold, Steven M. "MAC/GMC 4.0 User's Manual-Keywords Manual", NASA/TM-2002021 2077/VOL2

Bednarcyk, Brett A.; Arnold, Steven M, "MAC/GMC 4.0 User's Manual-Example Problem Manual", NASA/TM-2002021 2077/VOL3

Bednarcyk, Brett A., "Modeling Woven Polymer Matrix Composites With MAC/GMC", NASA/CR—2000-210370

Bhatt, Ramakrishna T.; Choi, Sung R.; Cosgriff, Laura M.; Fox, Dennis S.; Lee, Kang N., "Impact Resistance of EBC Coated SiC/SiC Composites". NASA/TM—2008-214406, ARL-TR-0646. October 2008

Brewer David, "HSR:EPM combustor materials development program", Materials Science and Engineering A261 (1999) 284–291

Chawla, K.K. "CERAMIC MATRIX COMPOSITES". Chapman & Hall.1993

Choi, S. R., "Foreign Object Damage Phenomenon by Steel Ball Projectiles in a SiC/SiC Ceramic Matrix Composite at Ambient and Elevated Temperatures", J. Am. Ceram. Soc., 91 [9] 2963–2968 (2008)

Choi , S. R.; Alexander, D. J., "Foreign Object Damage by Steel Ball Projectiles in a SiC/SiC Ceramic Matrix Composite at Ambient and Elevated Temperatures", Technical Report, Naval Air Warfare Center Aircraft Division, Report No: NAWCADPAX/TR-2008/3. 2008

Department of Defense Handbook 17-5, Composite Materials Handbook, volume 5 cermanic matrix composites

General Electric, "EEE High pressure turbine test hardware detail design report " NASA CR-167955

Gowayed, Y.; Ojard, G.; Miller, R.; Santhosh, U.; Ahmad, J. ; John, R. "Mechanical Properties of MI SiC/SiC Composities and their Constituents" AFRL-ML-WP-TP-2007-472, 2007

Jones, Eric L., "Overview of RXS Ceramic Composite Activities". Conference proceedings. HBCU/MI STEM Collaboration Symposium, Dayton, OH. July 8th, 2010

Kim, Ted T., "THERMO-MECHANICAL CHARACTERIZATION OF SILICON CARBIDE-SILICON CARBIDE COMPOSITES AT ELEVATED TEMPERATURES USING A UNIQUE COMBUSTION FACILITY", Dissertation, Department of the air force, air university. Wright-Patterson Air Force Base, Ohio

Macek, R. W.; Silling, S.A.,"Peridynamics via Finite Element Analysis," Finite Element Analysis and Design, Vol. 43, 2007, pp. 1169-1178

Mital, Subodh K. ; et al, "modeling of Melt-Infiltrated SiC/SiC composite properties", NASA/TM-2009-215806

Ogi, Keiji; Okabe, Tomonaga; Takahashi, Manabu; Yashiro, Shigeki; Yoshimura, Akinori; Ogasawara, Toshio, "Experimental characterization of high-speed impact damage behavior in a three-dimensionally woven SiC/SiC composite". Composites: Part A 41 (2010) 489–498

Silling, S. A., "Reformulation of Elasticity Theory for Discontinuities and Long-Range Forces," Journal of Mechanics and Physics of Solids, Vol. 48, 2000, pp. 175-209.

Silling, S.A.; Askari, E. , "A Meshfree Method Based on the Peridynamic Model of Solid Mechanics," Computers and Structures, Vol. 83, 2005, pp. 1526-1535.

Appendix A: Time dependent PD results

Damage progression in partially supported SiC/SiC CMC subjected to a steel impactor - 400m/s

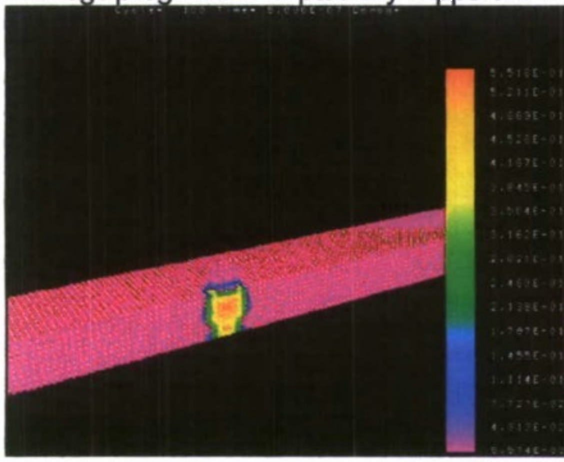

100 time step

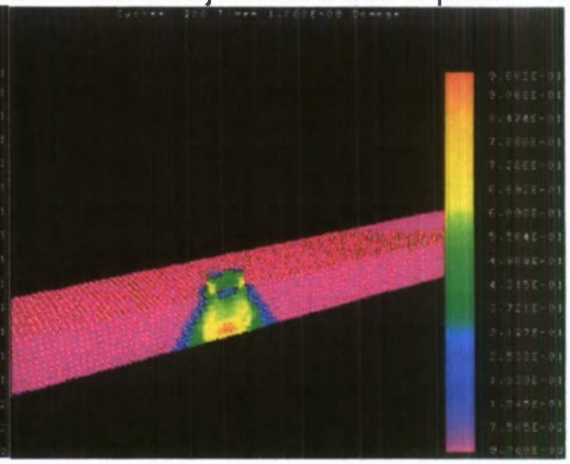

200 time step

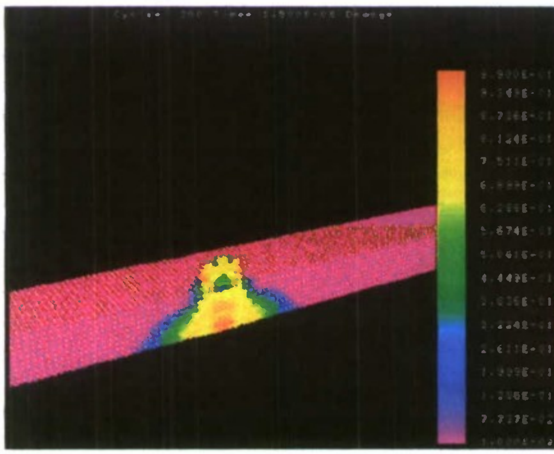

300 time step

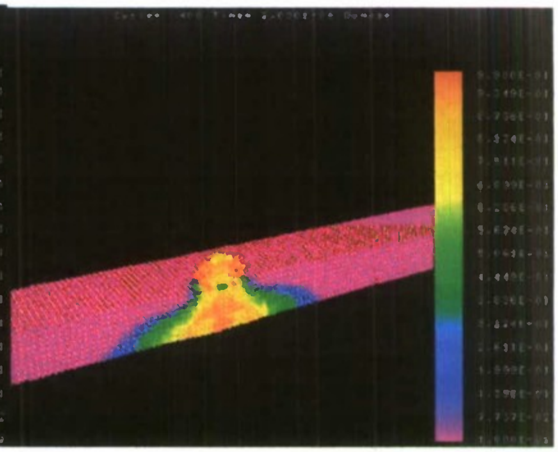

400 time step

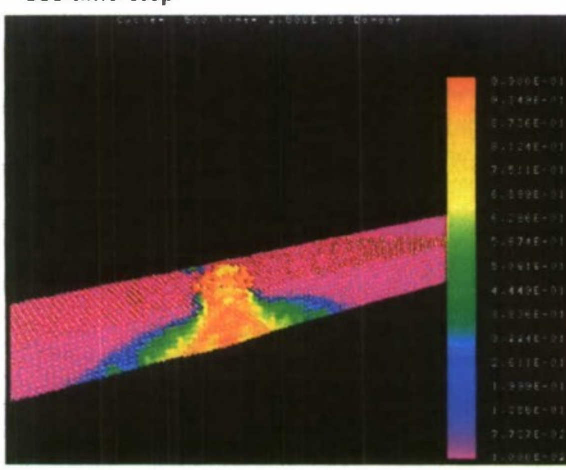

500 time step

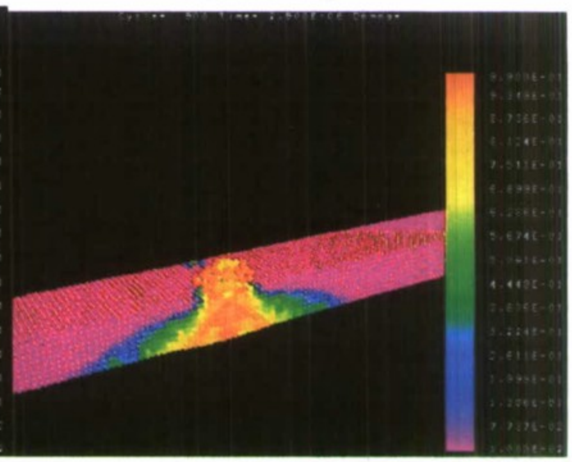

600 time step

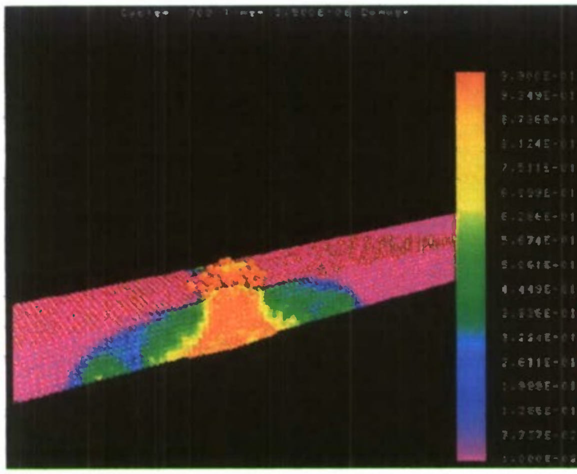

700 time step

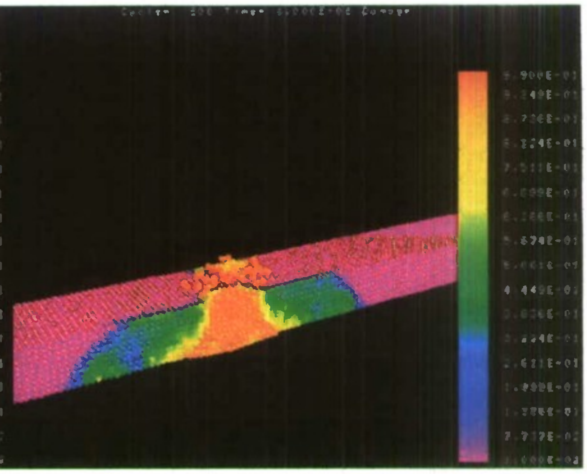

800 time step

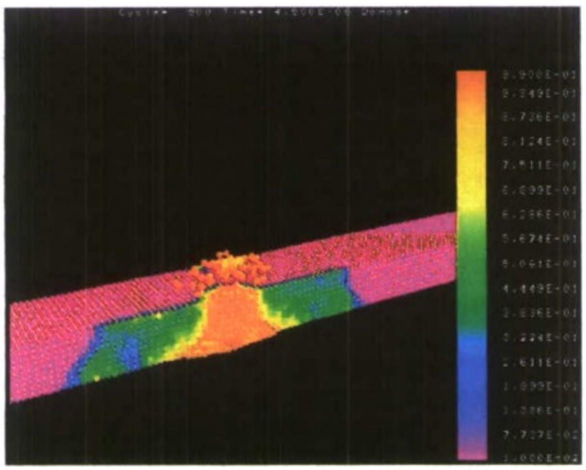

900 time step

[1] COI Ceramics, Inc.